THREE POINT BENDING AND UNI-AXIAL TENSION TESTS OF DOUBLE HOOK-END FIBERS

REMPLING Rasmus [1], FALL David , LUNDGREN Karin

Abstract

*This paper presents experimental results from tree point bending and uni-axial tension tests of fiber reinforced concrete, using steel fibers with a moderate fibre content (Vf = 0.3 %) of double hook-end steel fibres. The three-point bending tests included six notched fiber reinforced concrete (150mm*150mm*550mm) and six non-reinforced concrete beams and the uni-axial tension tests included six fiber reinforced- and six non-reinforced notched concrete cylinders that were core-drilled, 100mm, from rectangular specimens, >1000mm, and cut to 100mm lengths. The results from the beam tests show a separation of response into two groups of three beams with regard to the energy absorption capacity. Three beams showed relative low and three beams showed high capacity in comparison with other types of fibers. The results from the uni-axial tension tests showed a similar behaviour, but with a smaller scatter.*

Keywords: three point bending test, uni-axial tension test, fibre reinforced concrete, double hook-end fibre

1. Introduction

Extensive research has proven that steel fibre reinforcement provides significant post-crack ductility to the otherwise brittle concrete. This effect have been quantified in numerous studies [1, 2] and later also standards for assessment of the characteristic material parameters, e.g. fracture energy [3, 4]. Approximately a decade ago the Rilem technical committee 162-TDF, “Test and design methods for steel fibre-reinforced concrete”, published recommendations for two test methods: uni-axial tension test (UTT) and a three point bending test (3PBT) that can be used for assessing material parameters, see [3, 4]. In 2006, researchers from Gothenburg investigated these methods and compared them with an alternative method: the wedge-splitting test method. The investigation found that the scatter in the test results of all three tests was rather large due to variations in fibre distribution and orientation; and concluded that it is always necessary to count and explicitly state the number of fibres crossing the fracture plane, see [5].

[1] Rempling, Rasmus, Chalmers University of Technology, Civil and Environmental Engineering, Structural Engineering, Sven Hultins Gata 8, 412 96 Gothenburg, rasmus.rempling@chalmers.se

In this study the double hook-end fibre is assessed according to [3, 4]. The results from the uni-axial tension tests and the three point-bending tests are used for calculating the fracture energy of a fibre reinforced concrete mix with a fibre dosage of 35 kg/m^3.

2. Experimental program

2.1 Material data

Casting was made in the concrete laboratory of Chalmers University of Technology and the concrete was delivered from a ready-mix plant. All specimens were cast at one occasion and all concrete was from one of two batches: one with and one without steel fibres. Both mix compositions can be seen in Table 1.

Tab.1: Concrete mixes

Constitutents		Plain concrete [kg/m^3]	Fibre reinforced concrete [kg/m^3]
Cement	CEM II/A-LL Byggcement	338	322
Filler	Limus 4 Kalkstensfiller	179.5	178.3
Sand	0/4 Sjösand	741	728
Sand	0/8 Hol (Natursand)	170	163
Stone	4/8 Tagene (kross)	103	123
Stone	8/16 Tagene (kross)	616	621
Superplasticiser	Glenium 51/18 (BASF)	6.39 (2%)	6.41 (2%)
Air entraining agent	MicroAir100 1:10 (BASF)	0.47 (0.15%)	0.48 (0.15%)
Fibre			35
Water		182.6	172.9

2.2 Experimental set-up of uni-axial tension test

For each concrete type (conventional concrete and steel fibre reinforced concrete) six specimens were prepared and tested in uniaxial tension. The cylinders tested had a length of L = 100mm and a gross diameter of d =100mm. At the midsection of the cylinder a 10mm deep and 5mm wide circumferential notch was cut with a diamond blade. Six cylinders were cored from larger prisms 200x200x750mm3. The prisms were cast horizontally, see Figure 1. The top and bottom surfaces were face ground to ensure their being plane parallel.

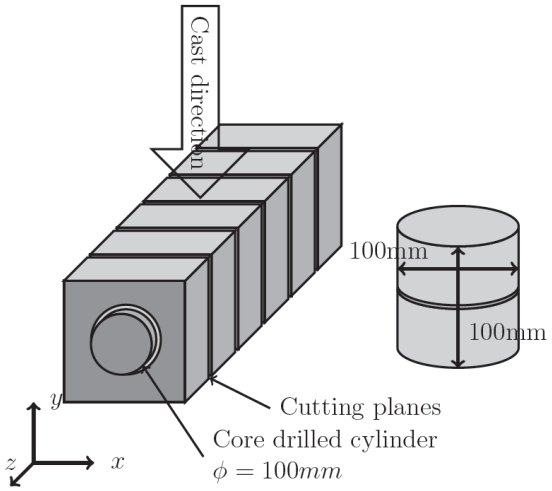

Fig.1: Making of cylinders for uni-axial tension tests.

The lower loading plate (metal block) was glued to the cylinders in a rig which ensured that the centre axes of the plate and the cylinder would coincide. The lower loading plate (together with the gluedon cylinder) was then bolted to the machine, and the upper loading plate, which was already attached to the machine, was glued to the top of the cylinder. Any small deviations from the edges of the cylinder being parallel to each other were evened out by the glue, so that the loading plates were positioned parallel to each other.

The direct tensile test setup was based on the test method recommended for concrete described in [4]. The tests, which were displacement controlled, were carried out in a GCTS servo hydraulic machine with a stiff load frame. The tests were conducted using a moment stiff loading device in order to suppress rotations of the holders that could lead to bending failure. The device was pretensioned with a load of 150kN. The load cell used was rated up to 200kN and the accuracy of the load measurement was within 1%. The displacement was measured locally over the notch with three inductive displacement transducers with a gauge length of 30mm. The gauges were approximately centered over the location of the notch. The transducers had a measuring range of _2.50mm and a relative error less than 1%. The mean value of the three displacement values was used for the displacement control. The displacement was applied at a rate of 0.005mm/min up to a displacement of $\delta = 0.1$mm, 0.1mm/min in the range $0.1 < \delta < 2.0$mm, and then increased to 0.5mm/min for the remaining part of the test. In Figure 2 the test setup is shown.

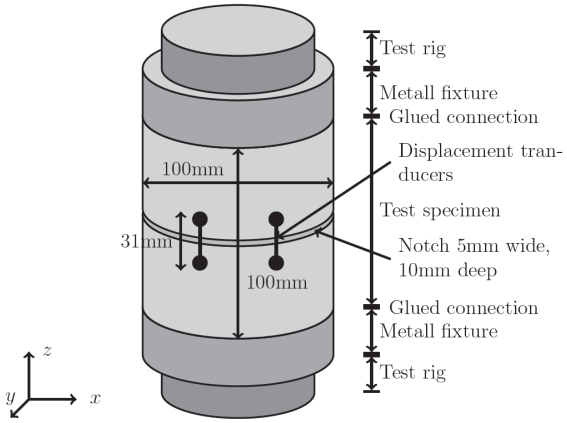

Fig.2: Test set-up of uni-axial tension test.

2.3 Experimental set-up of three point bending test

In addition to the uniaxial tensile testing presented in the previous section, three point bending tests, in accordance with [3], were made. The test set-up can be seen in Figure 3. In addition to the two linear variable differential transformers (LVDT) measuring the deflection on the top surface, the crack mouth opening displacement (CMOD) was recorded using a MTS 632 clip gauge. Both LVDT:s were RDP D2/200A with a range of ±5mm. All instrumentation was logged with a frequency of 100Hz. The beams were casted using buckets taking the concrete from the pumping truck. Casting was made in accordance with [3].

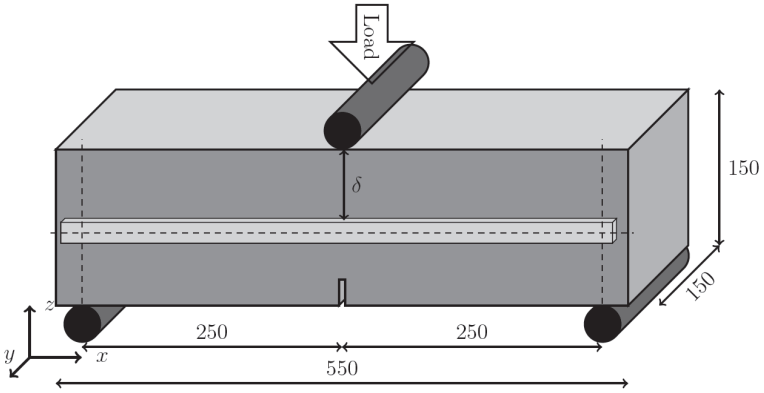

Fig.3: Test set-up of three point bending test.

3. Results

3.1 Results from uni-axial tension test and calculation of energy absorption capacity

Results from the tests on plain concrete and fibre reinforced concrete are shown in Figure 4 and Figure 5, respectively. Comparing the two graphs, the difference between the ductile fibre reinforced concrete and the brittle concrete is obvious.

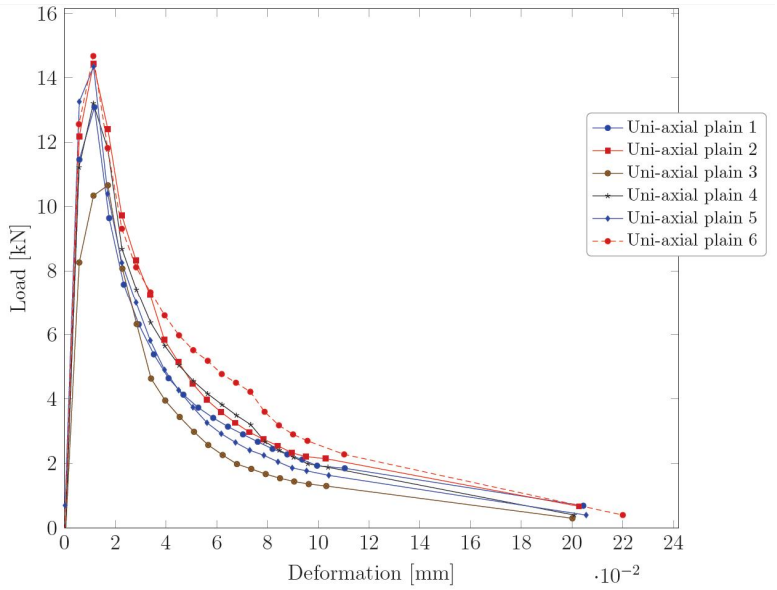

Fig.4: Load-deformation curve from uni-axial tension tests of plain concrete.

The uni-axial tension tests of plain concrete and fibre reinforced concrete gave results as expected. In two test specimens, a crack developed outside the notch, but after the initial crack in the notch, specimen 1 and 3. This gave a sudden drop in tensile hardening phase.

The number of fibres in the cracked section were calculated and observed, see table in Figure 5. Two specimens showed a larger amount of fibers, specimen 3 and 4. This high amount of fibres showed a corresponding high tensile hardening behaviour in the load-deformation curve.

Many fibres did not slip, instead they cleaved the surrounding concrete in a spalling way. The cleaving fibres were mostly joined in a sheaf of fibres.

In all specimens sheafs were found. The most extreme was specimen 5, in which 4 sheafs were counted including 10 fibers of 19 in all. These sheafs were also found to have cleaved the specimen; specimen 5 showed the lowest tensile hardening capacity, as well as the lowest energy absorption capacity.

The values from the tests on fibre reinforced concrete presented in Figure 5 were used for calculating the energy absorption capacity presented in Table 2. The calculation was according to [4].

A mean energy absorption capacity was calculated to $W_{f,mean}$ = 3.552 [N/mm]. The side crack developed in specimen 1 and 3 had no effect on the calculated energy absorption capacity, W_f = 3.236 [N/mm] and W_f = 4.661 [N/mm], for specimen 1 and 3, respectively.

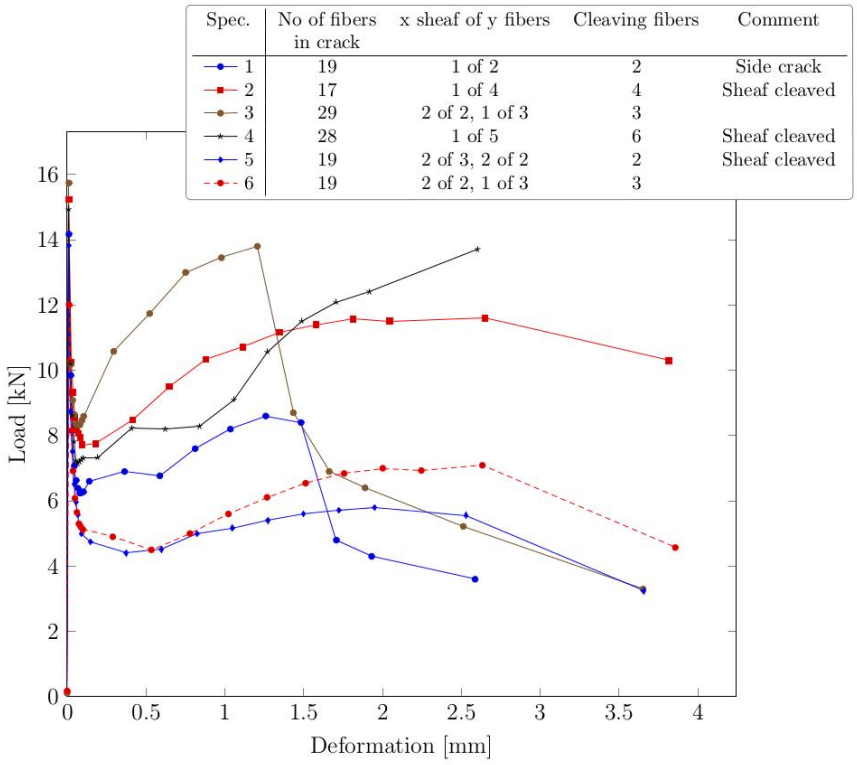

Fig.5: Load deformation curve from uni-axial tension tests of fibre reinforced concrete.

Tab.2: Energy absorption capacities from uni-axial tension tests. The capacities are calculated from load-deformation curves presented in Figure 5.

Uni-axial tension test	P_p[kN]	σ_p[MPa] $\frac{P_p}{A_n}$	w_i[mm]	W_f[N/mm] $\int_{w_i}^{w_m} \sigma_w(w)dw$
1	14.2	1.070	0.012	3.236
2	15.4	1.160	0.010	4.330
3	15.8	1.190	0.011	4.661
4	15.0	1.130	0.011	4.248
5	14.2	1.070	0.009	2.349
6	13.1	0.987	0.011	2.487

3.2 Results from three point bending test and calculation of energy absorption capacity

The results from the three point bending tests are shown in Figure 6 and Figure 7. The significant increase of ductility from steel fibres, seen in the uni-axial tension tests is observed also here. The significant difference between the fibre reinforced concrete beams are highly depending on the number of fibres bridging the crack. Furthermore, also the position of the fibre bridging the crack and the angle of the bridging fibre influences the residual capacity of the beam. Together with the graph, the numbers of fibres in the fracture zone of all beams are presented. A significant difference in number of fibres (and their position) could be observed, corresponding to the difference in residual capacity.

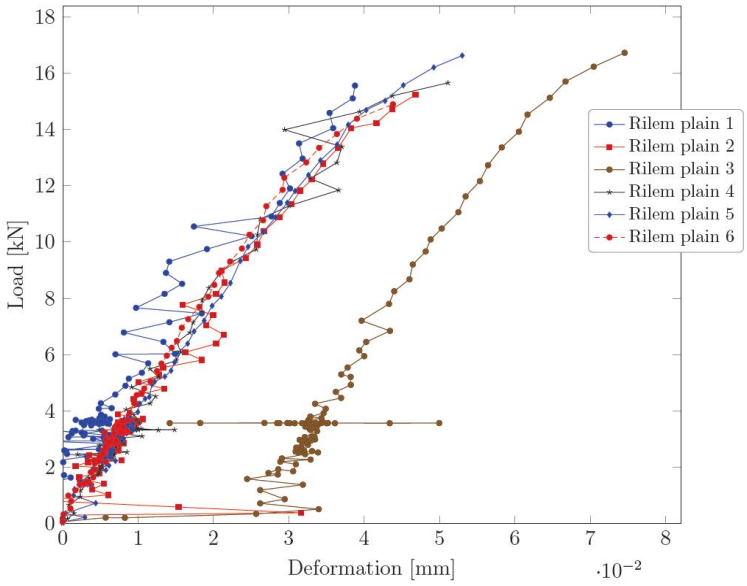

Fig.6: Load deformation curve from three point bending test of plain concrete.

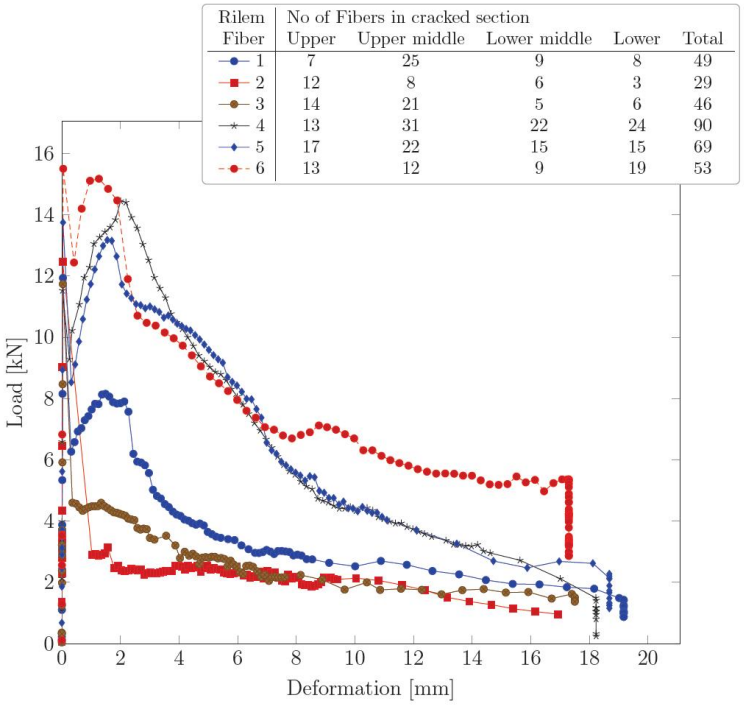

Fig.7: Load deformation curve from three point bending tests of fibre reinforced concrete

The values from the tests on fibre reinforced concrete presented in Figure 7 were used for calculating the energy absorption capacity presented in Table 4. The calculation was made according to [3].

Two capacities were calculated, $D_{BZ,2}$ *and* $D_{BZ,3}$, at two different deformations, δ_2 and δ_3, respectively. Specimen 2 showed a very low tensile hardening capacity which resulted in low energy absorption capacity.

The difference in number of fibres and their position reflected in the load-deformation curve results in a large difference in energy absorption capacity. The capacity is doubled for the specimen with a higher number of fibres in the lower section. However, a high number of fibers in the lower middle section seems not to have any effect on the energy absorption capacity.

Tab.3: Limit of proportionality and deformations from three point bending tests. The values are used for calculating the energy absorption capacity given in Table 4.

Rilem Fiber	F_L[kN]	δ_L[mm]	M_L[MN mm] $\frac{F_L}{2}\frac{L}{2}$	$f_{fct,L}$[N/mm^2] $\frac{3F_L L}{2bh_{sp}}$	δ_2[mm] $\delta_L + 0.650$	δ_3[mm] $\delta_L + 2.650$
1	13.0	0.048	1.625	520	0.698	2.698
2	14.0	0.043	1.750	560	0.693	2.693
3	13.0	0.045	1.625	520	0.695	2.695
4	14.1	0.078	1.763	564	0.728	2.728
5	14.0	0.046	1.625	560	0.696	2.696
6	15.5	0.049	1.763	620	0.699	2.699

Tab.4: Energy absorption capacities from three point bending tests. The capacities are calculated from load-deformation curves presented in Figure 7.

Rilem	$D_{BZ,2}$[kN mm]	$D_{BZ,3}$[kN mm]
1	2.906	17.877
2	nan	5.148
3	2.156	10.686
4	5.160	32.159
5	4.591	28.465
6	6.973	34.400

4. Conclusions

The following conclusions were drawn:

- Six uni-axial tension tests of plain concrete and fibre reinforced concrete reinforced with double hook-end fibres have been done according to Rilem standard, [4].
- Six three point-bending tests of plain concrete and fibre reinforced concrete reinforced with double hook-end fibres have been done according to Rilem standard, [3].
- The energy absorption capacity of double hook-end fibres has been calculated for the uni-axial tension tests and the three point bending tests according to [3] and [4].
- Steel fibres, just as expected, provide a significant addition in terms of ductility.
- A large amount of fibres were not separated in the mix. This resulted in a large amount of sheafs of fibers with consequences on the tensile hardening performance.
- The calculated energy absorption capacity was not affected to high extent of sudden drops, due to side cracks, in the tensile hardening phase.
- Many cases of cleavage were found in the cracked sections. This most probably affect the tensile hardening negatively as the crack development becomes more brittle.
- A high number of fibers in the lower section of the three point bending tests gave a high energy absorption capacity. Though, on the contrary, a high number of fibres in the lower middle section was found to not affect the energy absorption capacity.

Acknowledgements

This research was funded by the European Community´s Seventh Framework Programme under grant agreement NMP2-LA-2009-228663 (TailorCrete). More information on the project TailorCrete can be found at www.tailorcrete.com.

References

[1] Barros, J.A.O. and Figueiras, J.A., *Flexural behavior of SFRC: Testing and modeling.* Journal of Materials in Civil Engineering, 1999. 11(4): p. 331-339.

[2] Vandewalle, L., *Cracking behaviour of concrete beams reinforced with a combination of ordinary reinforcement and steel fibers.* Materials and Structures/Materiaux et Constructions, 2000. 33(227): p. 164-170.

[3] RILEM TC 162-TDF, *Bending test.* Materials and Structures, 2002. 35(9): p. 579-582.

[4] RILEM TC 162-TDF, *Uni-axial tension test for steel fibre reinforced concrete.* Materials and Structures, 2001. 34(1): p. 3-6.

[5] Löfgren, I., *Fibre Reinforced Concrete for Industrial Construction*, 2005, Department of Civil and Environmental Engineering, Chalmers University of Technology, Gothenburg, Sweden.